Australian Centre for Field Robotics
A Key Centre of Teaching and Research

The Rose Street Building J04
The University of Sydney 2006 NSW Australia

Sensor Data Integrity

Multi-Sensor Perception for Unmanned Ground Vehicles

Thierry Peynot, Sami Terho & Steve Scheding

T: + 61 2 9036 9193
E: t.peynot@acfr.usyd.edu.au

Technical Report ACFR-TR-2009-002

1 March 2009
Released 13 March 2009

Abstract

This document describes large, accurately calibrated and time-synchronised datasets, gathered in controlled environmental conditions, using an unmanned ground vehicle equipped with a wide variety of sensors. These sensors include: multiple laser scanners, a millimetre wave radar scanner, a colour camera and an infra-red camera. Full details of the sensors are given, as well as the calibration parameters needed to locate them with respect to each other and to the platform. This report also specifies the format and content of the data, and the conditions in which the data have been gathered. The data collection was made in two different situations of the vehicle: static and dynamic. The static tests consisted of sensing a fixed 'reference' terrain, containing simple known objects, from a motionless vehicle. For the dynamic tests, data were acquired from a moving vehicle in various environments, mainly rural, including an open area, a semi-urban zone and a natural area with different types of vegetation. For both categories, data have been gathered in controlled environmental conditions, which included the presence of dust, smoke and rain. Most of the environments involved were static, except for a few specific datasets which involve the presence of a walking pedestrian. Finally, this document presents illustrations of the effects of adverse environmental conditions on sensor data, as a first step towards reliability and integrity in autonomous perceptual systems.

The corresponding data are located at the following address:

`http://sdi.acfr.usyd.edu.au/`

Acknowledgments

This project was supported by the US Air Force Research Laboratory (Robotics Research Group), Tyndall, Florida, and the ARC Centre of Excellence programme, funded by the Australian Research Council (ARC) and the New South Wales State Government.
The authors of this document would also like to thank Craig Rodgers, Marc Calleja, James Underwood, Andrew Hill and Tom Allen for their valuable contribution to this work.

Contents

List of Figures

1 Introduction

This project presents the first step towards developing and understanding integrity in perceptual systems for UGVs (Unmanned Ground Vehicles). Important issues addressed include;

- When do perceptual sensors fail, and why?
- What combination of sensors would be appropriate for a given operational scenario?
- Can perceptual sensor failure be reliably detected and mitigated?

Failure is a very broad term; it is hoped that through this work a UGV systems designer will have a better understanding of exactly what constitutes perceptual failure, how it may be designed for and its effects remediated. Such failures would not just include hardware failure, but also adverse environmental conditions (such as dust or rain), and algorithm failure.

To begin to address these issues, synchronised data have been gathered from a representative UGV platform using a wide variety of sensing modalities. These modalities were chosen to sample as much of the electromagnetic spectrum as possible, with the limitation that the sensors be feasible (and available) for use on UGVs. A preliminary analysis has then been performed on the data to ascertain the prime areas of competence of the sensors, and the combination of sensors most promising for a set of representative UGV scenarios.

Further work (not contained in this document) would develop the theoretical framework for sensor data-fusion and on-line integrity monitoring for use in UGV perceptual systems. In particular, the latter would provide an on-line "quality" evaluation of the environment perception and/or the environment modeling based on that perception [6], with sensor/modeling fault detection and isolation [5, 4]. This would constitute a substantial benefit for UGV navigation efficiency, robustness and safety.

This document is structured as follows: the first chapter presents the system used to gather the data, in particular the sensors involved (and their characteristics). The second chapter presents the datasets collected, listing the kind of environment, the conditions and the relevant information to be able to exploit the data. Finally, the third chapter gives a preliminary analysis of sensor data integrity, based on the gathered data.

2 Presentation of the System

This chapter presents the system used to collect the data. It is composed of a ground vehicle called the Argo, equipped with various sensors.

2.1 The Argo vehicle

The vehicle used to collect the data, the CAS[1] Outdoor Research Demonstrator (CORD), is an 8 wheel skid-steering vehicle with no suspension (see Fig. 1), which turns thanks to pressure controlled brakes on both sides. It has a petrol engine, with a 12V alternator, and a 24V alternator to provide power to the computers and sensors on board.

For the purpose of this work, it has been equipped with multiple sensors, described in the following section.

2.2 The Sensors

All exteroceptive sensors are mounted on a sensor frame on top of the vehicle, as can be seen on Figures 1 and 2.

2.2.1 Laser Range Scanners

Four laser range scanners are used. Two of them are SICK LMS 291, they are mounted at the centre of the sensor frame. The two others are SICK LMS 221 mounted on both sides of that frame. The approximate configuration of these lasers, together with the names that will be used in the rest of this document, are the following[2] (see Fig. 2. Note that *roll* corresponds to a rotation around axis X and *pitch* to a rotation around axis Y):

[1] CAS stands for *Centre for Autonomous Systems*

[2] see Section 2.2.5 on calibration for more precise estimation of their positions on the vehicle

Figure 1: The Argo Vehicle

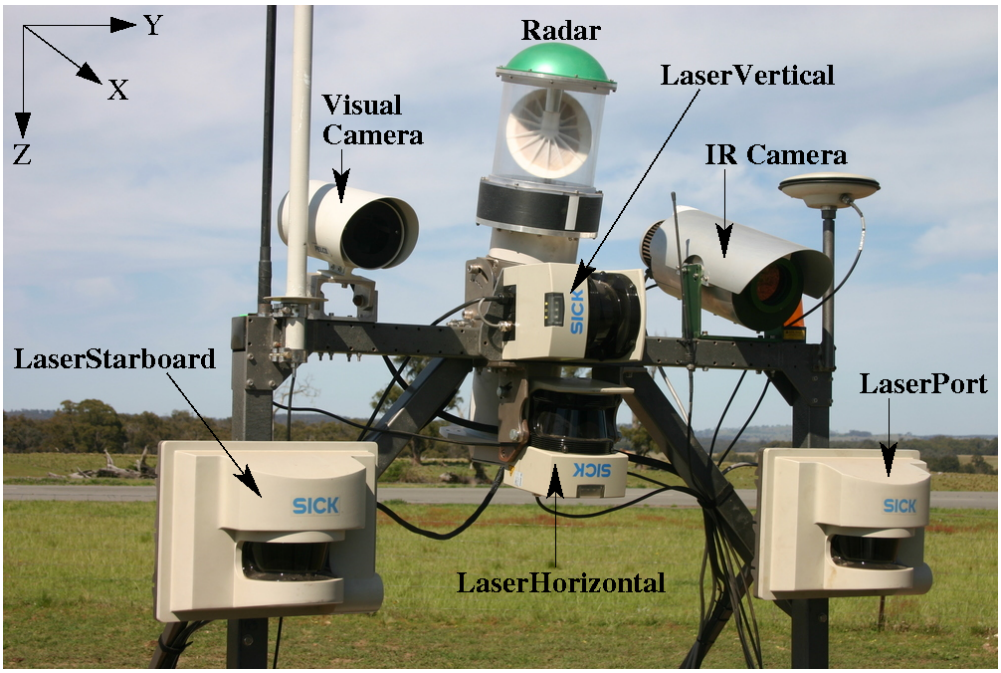

Figure 2: Argo Sensor Frame

1. *LaserHorizontal*: centered on the sensor frame, slightly pointing down to the ground (a few degrees of pitch), zero roll[3].
2. *LaserVertical*: centered on the sensor frame, with 90 degrees roll (thus scanning vertically), zero pitch.
3. *LaserPort*: located on the Port side of the vehicle, this laser is slightly pointing down to the ground (a few degrees of pitch, less than for the *LaserHorizontal*), zero roll.
4. *LaserStarboard*: located on the Starboard side of the vehicle, this laser is intended to have zero pitch and zero roll.

Characteristics and Nominal Performances

All four lasers were set to acquire data in the following mode:

- 0.25 degree resolution
- cm accuracy[4]
- 180 degree angular range[5]

2.2.2 FMCW Radar

This is a 94GHz Frequency Modulated Continuous Wave (FMCW) Radar (custom built at ACFR for environment imaging). Maximum rotation of scan head: 360 degrees at approximately 8Hz, 1KHz sample rate.

- Range resolution: $0.2m$.
- Maximum range: $40m$.

2.2.3 Visual Camera

The *Visual* camera (as opposed to the Infra-Red Camera) is a Prosilica Mono-CCD megapixel Gigabit Ethernet camera, pointing down (a few degrees of pitch).

Characteristics and Nominal Performances

- Image Pixel Dimensions: 1360×1024
- Resolution: 72×72 ppi (pixels per inch)
- RGB Colour, depth: 8 bits

Operating Mode (Camera Parameters)

The camera was set up with the following parameters (see [8] for more details on the camera parameters):

- Nominal Framerate: 15 images per second in *static*[6] datasets, 10 images per second in *dynamic* datasets (unless specified differently).
- Exposure Mode: Automatic
- Gain Mode: Manual (Gain = 0 for all daytime tests, Gain = 20 for nighttime tests).
- Pixel Format: *Bayer8* [8]
- White Balance: *AutoOnce* (i.e. an automatic white balance is made at the very beginning of an image acquisition sequence, determining the offsets once and for all, then the white balance mode is set to *Manual* with these constant values).

[3]Note that this laser looks flipped over on Fig. 2 (i.e. 180 deg. roll). However, this is accounted for in the process of data acquisition, thus it should be considered as with a zero roll.

[4]except for the *cameras to lasers* calibration dataset, where the mm accuracy mode was used for more precision, but limiting the maximum range to 8m and the angular range to 100 degrees.

[5]except for the *cameras to lasers* calibration dataset, for which a 100 degree angular range was used.

[6]see section 4.2

2.2.4 Infra-Red (IR) Camera

The IR camera is a Raytheon *Thermal-eye 2000B*. Analog images are acquired through a frame grabber providing digital images of size 640×480 pixels.

Characteristics and Nominal Performances

- Image Pixel Dimensions of complete image: 640×480. In practice, though, the images are usually clipped to 511×398 to remove useless black bands on the sides[7](see Fig. 3). The actual sensor size is: 320×240.
- Average Framerate: 12.5 images per second (unless specified differently).
- Spectral response range: $7 - 14\mu m$.

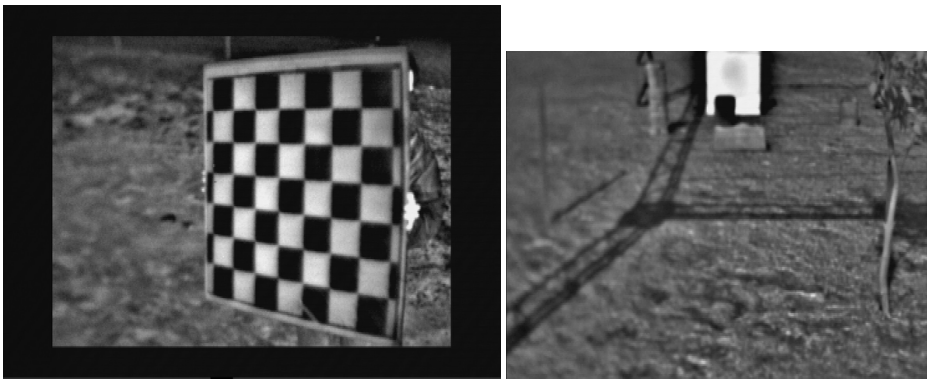

(a) Original image (from calibration dataset) (b) Clipped image (from dataset 14)

Figure 3: Examples of images from the IR camera

2.2.5 Calibration parameters

The spatial transformations between sensors and reference frames have been estimated using thorough calibration methods. The frames used are illustrated on Fig. 4. They are named:

- *Navigation frame*: (fixed) global frame defined by the three axis: $X^n = North$, $Y^n = East$ and $Z^n = Down$ in which positions are expressed in UTM coordinates (Universal Transverse Mercator).
- *Body frame*: frame linked to the body of the vehicle, its centre being located at the centre of the IMU (Inertial Measurement Unit), approximately at the centre of the vehicle. The axis are: X^b pointing towards the from of the vehicle, Y^b pointing to the Starboard side of the vehicle, and Z^b pointing down.
- *Sensor frame*: frame linked to a particular sensor. It is defined in a similar way as the previous one (i.e. X^s forward, Y^s starboard, Z^s down), but centered on the considered sensor.

Note that in the rest of the document *Navigation* (or localisation) will correspond to the global positioning of the *Body frame* in the *Navigation frame*.

The *measured* distances between sensors are illustrated in Fig. 5. Note that an actual process of calibration usually provides better estimations of the real transformations between sensors. However these measured values are good initial estimates for calibration processes (and they were actually used as such in this work).

Two categories of calibration have been made:

[7]except for the calibration dataset

- *Range Sensor Calibration*, to estimate the transformations between the frame associated to each range sensor (laser scanner or radar) and the *Body* frame.
- *Camera Calibration*, to estimate the intrinsic (geometric) parameters of each camera, and the extrinsic transformations between cameras and lasers.

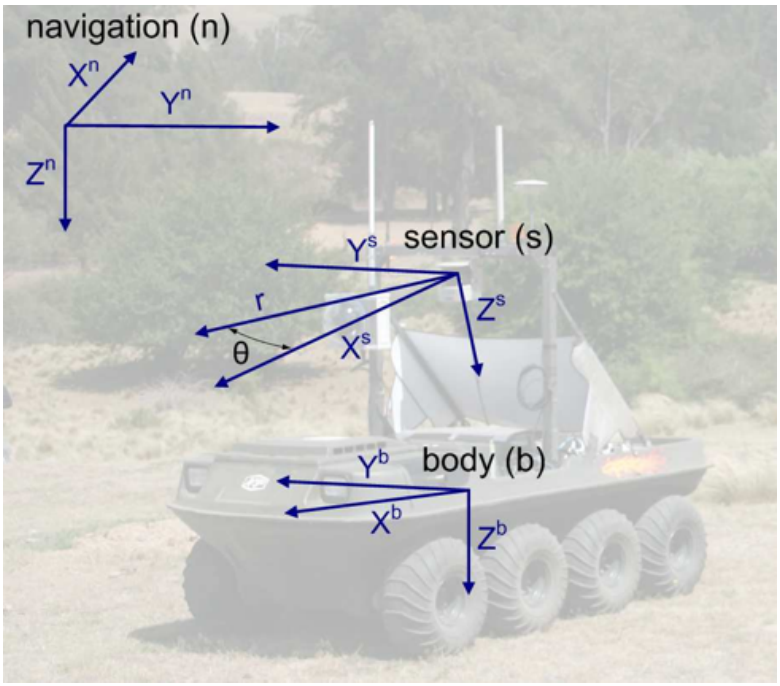

Figure 4: *Sensor*, *Body* and *Navigation* frames on the Argo

Range Sensor Calibration

The estimation of the transformations between the frame associated to each range sensor (laser scanner or radar) and the Body frame was made using a technique detailed in [1, 9]. For that purpose, a dataset was acquired in an open area with flat ground and key geometric features such as a vertical metallic wall, two vertical poles with high reflectivity for lasers, and two vertical poles for the radar (see section 4.4.2).

The results of this calibration are the estimation of the 3 rotation angles ($RollX$, $PitchY$ and $YawZ$) and 3 translation offsets (dX, dY, dZ) from the Body frame to the Sensor frame. All angles will be expressed here in degrees for convenience and distances in metres.

The following table shows the results obtained after combined calibration of all four range sensors, i.e. *LaserHorizontal* (or *LaserH*), *LaserVertical* (or *LaserV*), *LaserPort* (or *LaserP*), *LaserStarboard* (or *LaserS*) and the *Radar*. Common features are used for all sensors. Naturally, it is recommended to use such calibration parameters when combining the information from groups of these sensors.

Transformations Body Frame to Sensor Frame:

Sensor	RollX	PitchY	YawZ	dX	dY	dZ
LaserH	-0.732828	-8.586863	-1.631319	0.108987	0.008302	-0.919726
LaserV	88.562966	-0.118007	-1.123153	-0.000291	-0.082272	-1.126802
LaserP	-0.500234	-2.616210	-1.805911	0.190857	-0.548777	-0.763776
LaserS	-0.608178	-0.431051	-2.349991	0.198663	0.534253	-0.849538
Radar	-0.151571	191.161703	173.278081	-0.025753	-0.047174	-1.399104

Visual Camera Calibration

Intrinsic parameters The *intrinsic* calibration of each camera was made using the *Camera Calibration Toolbox for Matlab* [2]. The following is the content of the `Calib_Results.m` file exported by the

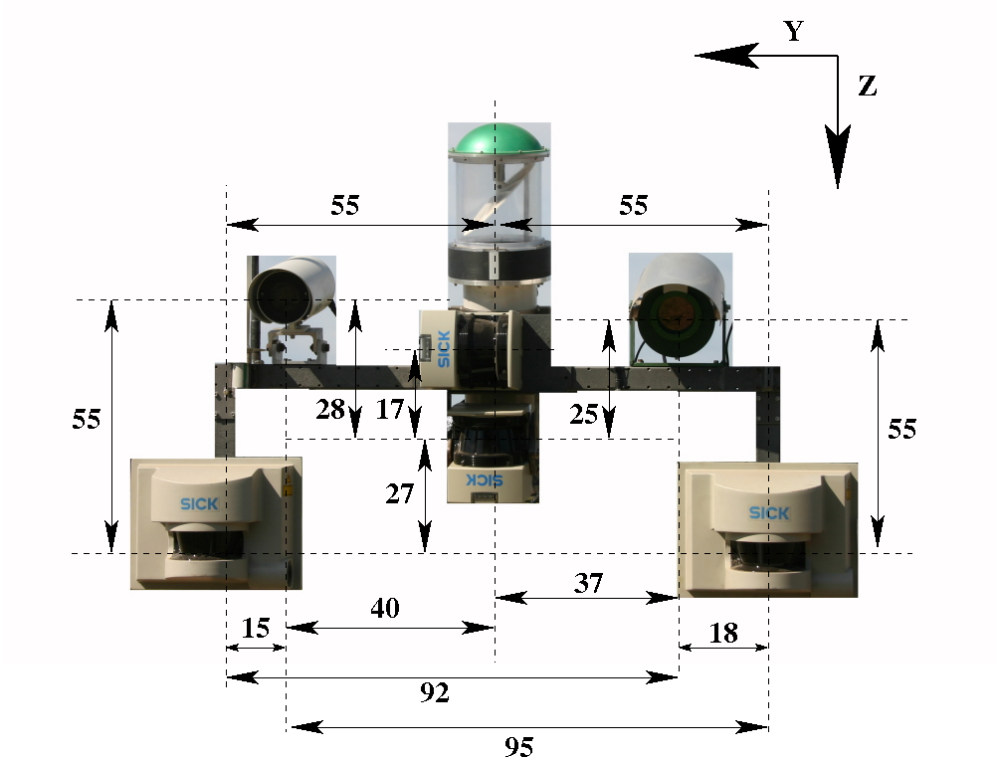

Figure 5: Distances between sensors in the (y,z) plane, in cm. Note that the dashed lines are meant to go through the centre of the sensors (despite any other impression due to perspective of the original picture).

toolbox, that describes the output of the calibration process in Matlab language:

```
%-- Focal length:
fc = [1023.094873083798120; 1020.891695892045050];
%-- Principal point:
cc = [643.139025535655492; 482.455417980580421];
%-- Skew coefficient:
alpha_c = 0.000000000000000;
%-- Distortion coefficients:
kc = [-0.218504818968279; 0.138951469767851;
      -0.000755791245166; 0.000175881419552; 0.000000000000000];
%-- Focal length uncertainty:
fc_error = [1.240637187529808; 1.220702756108720];
%-- Principal point uncertainty:
cc_error = [1.338561085455541; 1.362301725972313];
%-- Skew coefficient uncertainty:
alpha_c_error = 0.000000000000000;
%-- Distortion coefficients uncertainty:
kc_error = [0.001808042132202; 0.003689996468947;
      0.000207366100112; 0.000221355286767; 0.000000000000000];
%-- Image size:
nx = 1360;
ny = 1024;
```

The reader is invited to consult the toolbox web site [2] for more details on these parameters. These output files from the calibration toolbox are included in the datasets, in the directory

`VisualCameraCalibration/Calibration`.

Note that of the 93 images selected for the calibration process, 74 were actually used in the final optimisation process (see the file `Calib_Results.m` for details). The pixel error obtained for this calibration is:

```
Pixel error:  err = [ 0.19209 0.20252 ]
```

Extrinsic parameters (position of camera with respect to lasers) The extrinsic transformations between each camera and each laser was made using a method adapted from [7]. It uses the ouput of the Matlab Camera Calibration Toolbox to estimate the positions and orientations of the planes corresponding to the checker board visible in the images. These positions are compared with the positions of the laser points hitting this board. An optimisation process gives an estimation of the position of the laser range scanner with respect to the camera.
The offset translations (δX_c, δY_c,δZ_c) and rotations (ϕX_c, ϕY_c,ϕZ_c), indicated in the tables below, describe how to move each laser so that it aligns with the camera. They are expressed in the camera frame, using the Matlab Toolbox convention (i.e. $+X_c$ to the right, $+Y_c$ down, $+Z_c$ forward, Fig. 6). Distances are expressed in metres and angles in degrees.

LaserHorizontal **to visual camera:**

δX_c	δY_c	δZ_c	ϕX_c	ϕY_c	ϕZ_c
0.4139	-0.2976	-0.0099	-4.7341	-0.3780	-0.4230

LaserVertical **to visual camera:**[8]

δX_c	δY_c	δZ_c	ϕX_c	ϕY_c	ϕZ_c
0.5045	-0.0905	-0.208	-13.2030	-0.5851	-0.3140

LaserPort **to visual camera:**

δX_c	δY_c	δZ_c	ϕX_c	ϕY_c	ϕZ_c
0.9592	-0.5011	-0.0867	-10.6026	-0.0747	-0.5791

LaserStarboard **to visual camera:**

δX_c	δY_c	δZ_c	ϕX_c	ϕY_c	ϕZ_c
-0.1343	-0.4976	-0.0532	-12.6652	0.2409	-0.5293

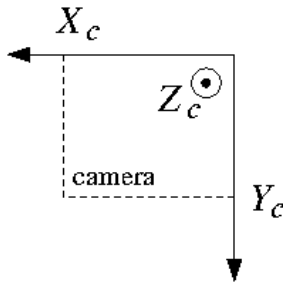

Figure 6: Camera Frame in the Matlab Calibration Toolbox

IR Camera Calibration

Intrinsic parameters The intrinsic calibration of this camera was also made using the *Camera Calibration Toolbox for Matlab* [2]. The following is the content of the `Calib_Results.m` file exported by

[8]Note that this transformation was computed by combining the previous transformation *LaserHorizontal to camera* with the relative transformation of the two lasers found in the Range Sensor Calibration above, as the direct calibration method would not provide satisfying results. This means that this estimation is likely to be corrupted by a higher level of error.

the toolbox, that describes the output of the calibration process in Matlab language:

```
%-- Focal length:
fc = [790.131547995049573; 826.825751328548790];
%-- Principal point:
cc = [328.685823692670340; 164.376489311973216];
%-- Skew coefficient:
alpha_c = 0.000000000000000;
%-- Distortion coefficients:
kc = [-0.466898225930376; 0.246094535921152;
      0.011203533644424; -0.005108186223306; 0.000000000000000];
%-- Focal length uncertainty:
fc_error = [5.782890597916310; 6.015102913624340];
%-- Principal point uncertainty:
cc_error = [9.426499879136482; 10.292926183444356];
%-- Skew coefficient uncertainty:
alpha_c_error = 0.000000000000000;
%-- Distortion coefficients uncertainty:
kc_error = [0.026759198529728; 0.152385380407985
      0.002604709115691; 0.002243445036632; 0.000000000000000];
%-- Image size:
nx = 640;
ny = 480;
```

The output files from the calibration toolbox are included in the datasets, in the directory

`IRcameraCalibration/Calibration`.

Extrinsic parameters (position of cameras with respect to lasers) The same operations as for the visual camera were applied to determine the transformations between each laser and the IR camera, in the camera frame.

LaserHorizontal **to IR camera:**

δX_c	δY_c	δZ_c	ϕX_c	ϕY_c	ϕZ_c
-0.3391	-0.3278	0.0975	-6.5307	-1.2671	-2.1308

LaserVertical **to IR camera:**[9]

δX_c	δY_c	δZ_c	ϕX_c	ϕY_c	ϕZ_c
-0.2485	-0.1207	-0.0115	-14.9996	-1.4742	-2.0218

LaserPort **to IR camera:**

δX_c	δY_c	δZ_c	ϕX_c	ϕY_c	ϕZ_c
0.2090	-0.5400	0.0194	-12.7686	-1.0343	-2.3348

LaserStarboard **to IR camera:**

δX_c	δY_c	δZ_c	ϕX_c	ϕY_c	ϕZ_c
-0.8772	-0.5652	0.0584	-15.7179	-0.8259	-3.3619

Note that the images and correspondings laser scans which were used for this calibration are available in the directory named `IRcameraCalibration` (see section 4.4.1). The images in this dataset are full resolution 640×480 as provided by the frame grabber, unlike the IR images in the other datasets which are clipped to keep only the part containing actual information.

2.2.6 Additional Sensors

Other sensors available on the Argo platform that provide useful information are:

- a Novatel SPAN System (Synchronized Position Attitude & Navigation) with a Honeywell IMU (Inertial Measurement Unit). This usually provides a 2cm RTK solution for localisation,
- wheel encoders, measuring wheel angular velocities,
- brakes sensors (position and pressure),
- engine and gearbox rotation rate sensors.

[9]Note that, as for the Visual camera previously, this transformation was calculated by combining the previous transformation *LaserHorizontal to camera* with the relative transformation of the two lasers found in the Range Sensor Calibration above.

3 Data Format and Content

This chapter presents the format of the data provided. Section 3.1 describes the organisation of directories and files. Section 3.2 precisely defines the format of the content of each file containing data. Note that in the rest of the document the Typewriter font will be used to designate names of `directories` and `files` as well as `text` written in ASCII files.

3.1 Files and Directories Organisation

Each dataset has its directory containing all data from all sensors. It usually corresponds to a particular test (specific environment and conditions). Its name is composed of a number (corresponding to the chronological order of the data acquisition) and a string roughly describing the environment and conditions[10]. An example is: `04-StaticLightDust` for a *static*[11] test in the presence of light dust.

A regular dataset directory typically contains *ten* sub-directories corresponding to the differents sensors involved (or type of data, see section 2.2); namely:

- `LaserHorizontal`
- `LaserPort`
- `LaserStarboard`
- `LaserVertical`
- `Nav`
- `Payload`
- `RadarRangeBearing`
- `RadarSpectrum`
- `VideoIR`
- `VideoVisual`

3.2 ASCII Log File Description

This section describes the content of the ASCII files that can be found in each of the directories mentioned above. Note that in all logged ASCII files, the default units will be metres for all distances and radians for all angles (except for the *RadarSpectrum* data). Consequently, anywhere units are not clearly specified, metres and radians prevail. All files start with a time stamp, expressed in seconds, which corresponds to the *Unix* time.

Files contain one data sample (complete) message per line. The first columns of all ASCII file have the general form:

`*<timestamp> TEXT_TYPE data`

where `TEXT_TYPE` is a string describing the type of data written on this line (e.g. `NAV_DATA` for navigation data) and `data` is the actual data from the sensor, written on as many columns as needed.

More specifically, the next sections describe the actual content of each type of file for each type of sensor or data. They will first indicate the name of the directory where the data can be found and then illustrate the content by a table.

3.2.1 Navigation (Localisation)

Name of directory: `Nav`.
The ASCII data are contained in a file named `NavQAsciiData.txt`. The content of each line of this file is described in the following table. It corresponds to the global localisation of the vehicle (*Body frame*) expressed using the UTM coordinate system, in metres and radians; namely: the three translations (North, East, Down) and the three rotations around the same axis (RollX, PitchY, YawZ). Each line also shows the variations of these entities (dNorth, dEast, dDown, dRollX, dPitchY, dYawZ) and the

[10] a much more complete description is provided inside each directory though
[11] See the more precise definition of *static* and *dynamic* test in chapter 4.

corresponding covariances matrix.

Column:	1	2	3	4	5	6	7	8
Data :	*<timestamp>	NAV_DATA	North	East	Down	dNorth	dEast	dDown
Column:		9	10	11	12	13	14	15-158
Data:		RollX	PitchY	YawZ	dRoll	dPitch	dYaw	$C_{i,j}$

where $C_{i,j}$, $(i,j) \in [\![1,12]\!]^2$ are the elements of the covariance matrix describing the covariances between the 12 elements appearing in columns 3 to 14. Note that this matrix is written in rows: the whole row number 1 first, then row 2 etc... In other words, it is written as: $C_{1,1}, C_{1,2} \ldots, C_{1,12}, C_{2,1}, C_{2,2} \ldots C_{12,12}$.

3.2.2 Range Data from Lasers

This sub-section concerns the directories of the four lasers, namely:

- `LaserHorizontal`
- `LaserVertical`
- `LaserPort`
- `LaserStarboard`

In each of these directories, the ASCII data are contained in a file named `RangeBearingQAsciiData.txt`. The content of each line of this file is described in the following table. Each line of the file typically shows the result of a 2D scan of 180 degrees with an increment of 1 degree. The first part of the line gives parameters describing this scan and the second part gives the actual range values returned by the laser sensor. 4 successive scans (i.e. 4 lines in the file), with starting angles each time incremented by 0.25 degree, finally provide a full 180 degree wide and 0.25 degree resolution scan.

Column:	1	2	3	4
Data :	*<timestamp>	RANGE_DATA	StartAngleRads	AngleIncrementRads
Column:	5	6	7	$8 - end$
Data :	EndAngleRads	RangeUnitType	NScans	$\texttt{Range}_i$

where:

- `StartAngleRads` (*double*) is the value in radians of the first angle of the current scan (i.e. the one described on the current line of the file).
- `AngleIncrementRads` (*double*) is the difference of angle between two successive scan values (namely $\texttt{Range}_i$ and $\texttt{Range}_{i+1}$), in radians.
- `EndAngleRads` (*double*) is the value in radians of the last angle of the current scan (i.e. the current line).
- `RangeUnitType` is an integer showing the unit for the range values that follow in the line ($\texttt{Range}_i$). The possible integers and their meanings are as follow:
  - 1: mm
  - 2: cm
  - 3: m
  - 4: km
- `NScans` is the number N of scan values. Note that: $end = 8 + (\texttt{NScans} - 1)$
- $\texttt{Range}_i$, with $i \in [\![1, N]\!]$, are the actual range values for each angle of the current scan (the unit being determined by the value of `RangeUnitTypeEnum`).

3.2.3 Radar Spectrum

The directory: `RadarSpectrum` contains the radar spectrum, described as the bins of a Fast Fourier Transform (FFT). The ASCII data are contained in a file named `HSR_ScalarPoints1.txt`. The content of each line of this file is described in the following table:

Col.:	1	2	3 to end
Data:	`*<timestamp>`	`Angle`(degrees)	$\texttt{Reflectivity}_i$

where:

- `Angle` is the angle, in *degrees*, of the bins of this line.
- $\texttt{Reflectivity}_i$ with $i \in [\![1, N]\!]$ (N being the total number of bins on the line) are the reflectivities for each bin. Each of those bins corresponds to a different range, which can be determined using the following.

First, note the following parameters, obtained after intrinsic calibration of the radar scanner:

- the Sample Frequency is $sampleFreq = 1250000Hz$.
- the frequency per metre is: $hertzPerM = 4336.384Hz/m$.
- the range offset is: $offsetM = -0.3507m$.

Knowing those parameters, the range associated to a particular bin ($binRange$) can be found by calculating:

$$\begin{array}{ll} frequencyHzPerBin & = sampleFreq/(2 * numberOfBins) \\ rangeMPerBin & = frequencyHzPerBin/hertzPerM \\ binRange & = bin \times rangeMPerBin + offsetM \end{array} \quad (1)$$

where bin represents the bin number (i.e. column number in the file - 2, starting with 1) and $binRange$ is the range associated to this particular bin.

3.2.4 Range Data from Radar

This sub-section concerns the directory named `RadarRangeBearing`. It contains range information from the radar, which is estimated from the spectrum. The ASCII data are contained in a file named `RangeBearingQAsciiData.txt`. Its format is very similar to the laser files seen above, only with reflectivity information in addition to the range information. The content of each line of the file is described in the following table:

Col.:	1	2	3	4
Data:	`*<timestamp>`	`RANGE_REFLECTIVITY_DATA`	`StartAngleRads`	`AngleIncrRads`
Col.:	5	6	7	8
Data:	`EndAngleRads`	`RangeUnitType`	`NScans=1`	$\texttt{Range}_1$
Col.:	9			
Data:	$\texttt{Reflectivity}_1$			

where:

- `StartAngleRads` (double) is the value in radians of the first angle of the current scan (i.e. the one described on this line of the file).
- `AngleIncrRads` (double) is the difference of angle (increment) between two successive scan values. Typically, `AngleIncrRads` $= 0$ in this file, as there is only one range value per line.
- `EndAngleRads` (double) is the value in radians of the last angle of the current line. In practice, in this file: `EndAngleRads` $=$ `AngleIncrRads`.
- `RangeUnitType` is an integer showing the unit for the range values that follow in the line. The possible integers and their meanings are as follow:
  - 1: mm
  - 2: cm
  - 3: m
  - 4: km

- `NScans` is the number of scan values. Here `NScans`=1 (one range value per line only).
- $\texttt{Range}_1$ is the actual range value for the current angle of the current scan (the unit being determined by the value of `RangeUnitTypeEnum`).
- $\texttt{Reflectivity}_1$ is the reflectivity of this current bin.

The range and reflectivity information contained in this file are extracted from the FFT (see section 3.2.3) by searching for the peak of highest reflectivity. The corresponding range that can be calculated by direct application of equation (1) is limited to the resolution of the discrete FFT: $0.28m$. Thus, to obtain a higher accuracy, a quadratic interpolation is performed on the peak processed from the signal: the interpolated range is the range obtained for the maximum point of the quadratic polynomial that is fitted to the three points of the FFT spectrum defining the peak (see [3] for more details).

3.2.5 Camera Images

Two directories concern camera images: one for the Infra-Red Camera (`VideoIR`) and one for the Visual Camera (`VideoVisual`). Both contain the same type of data:

- One ASCII file named `VideoLogAscii.txt`, with the following format:

Column:	1	2	3
Data:	`*<timestamp>`	`VISION_FRAME`	`<filename>`

- One directory `Images` containing all the bmp images (as files) provided by the camera. Those files have the names described in the `VideoLogAscii.txt` file. Note that this name is formed by the prefix `'Image'` followed by a timestamp (where the '.' between seconds and fractions of seconds has been replaced by '`-0`'), plus the extension '`.bmp`'.

3.2.6 Vehicle Internal Data

Additional proprioceptive data can be found in the directory: `Payload`.
This concerns internal data from the vehicle, such as status of braking or wheel velocity. Note that this category of data is only relevant for the *dynamic* tests (moving vehicle). Thus they shall be found only for this category of datasets. The ASCII data are contained in a file named `PayloadData1.txt`. The regular format of each line of this file is still:

`*<timestamp> TEXT_TYPE data`

with `TEXT_TYPE` having various possible values. These values and the corresponding line format and content of `data` are described in the table below. Note that, as previously, the first line of this table shows the column number.

1	2	3	4
`*<timestamp>`	`SERVO_SETPOINT_DATA`	chokePosition	throttlePosition
`*<timestamp>`	`VELOCITY_TURN_RATE_DATA`	velocity	turnRate
`*<timestamp>`	`SENSOR_DATA`	`sensor`	`value`
1	2	3	4
`*<timestamp>`	`BRAKE_DATA`	leftBrakePosition	rightBrakePosition
		5	6
		leftBrakePressure	rightBrakePressure
1	2	3	4
`*<timestamp>`	`ACTUATOR_SETPOINT_DATA`	desiredChoke	desiredThrottle
		5	6
		desiredLeftBrake	desiredRightBrake

When `TEXT_TYPE` = `SENSOR_DATA`, `sensor` is an integer referring to a particular internal sensor. The possibilities and the corresponding meaning for `value` are illustrated in the following table:

sensor	value (unit)
0	Engine Rotation Rate (RPM)
1	Gearbox Rotation Rate (RPM)
2	12V Battery Voltage (V)
3	24V Battery Voltage (V)
4	Left Wheel Angular Velocity (rad/s)
5	Right Wheel Angular Velocity (rad/s)

Note that these data are provided for information, but a model of the vehicle would be needed to actually make the BRAKE_DATA, ACTUATOR_SETPOINT_DATA and the RPM information really useful for the reader. It is recommended to contact the authors in that case.

4 Datasets

There are two types of datasets. In the *static* ones the vehicle was stationary and the sensors were always acquiring data from the same fixed area. The area contained: features with known characteristics and dimensions inside an identified frame, and objects and equipment used for creating the environmental conditions (e.g. a compressor and a water pump), located outside of the frame. In the *dynamic* datasets the vehicle would be moving around the test area, which usually contained the same equipment as mentioned before, plus a car (from which the UGV was operated).

The purpose of the static datasets was to acquire data in different conditions but of a fixed scene, with the same features, to enable a comparison of the effects of different environmental conditions.

Note that *static* or *dynamic* will refer to the state of the vehicle, not the status of the environment, which can be considered as static in all datasets except when the presence of a moving element such as a *human* is explicitly mentioned.

The beginning and ending times of the datasets are expressed in three formats. The first column shows the Unix time, that is, seconds after midnight UTC of 1st January, 1970. The leap seconds are not counted in this convention. The second column shows the UTC time (Universal Timing Convention), equivalent to the Greenwich Meridian Time (GMT). The third column shows the local AEDT time in the test site. AEDT stands for: Australian Eastern Daylight Saving Time.

The data acquisition was made with several computers, all *accurately synchronised* using NTP (Network Time Protocol), allowing to have offsets between their internal times limited to a maximum of a few milliseconds. However, as some software applications were activated manually, sensor data logging was not necessarily starting at the exact same time for all sensors. Thus, for convenience, the indicated **Start** and **End** time correspond respectively to the earliest and the latest time of the dataset when all data from all sensors are available.

The next section describes each type of conditions that appear in the datasets.

4.1 Environmental conditions

The controlled environmental conditions include: presence of dust, smoke or rain.*Clear* environment, on the contrary, will mean absence of any of those adverse environmental conditions.

4.1.1 Dust

The dust was generated by blowing air to dusty soil. The blower was a high-power air compressor with a flexible tube for directing the air. Some of the datasets were gathered in areas where the soil was naturally very dusty. In these cases the dust was generated by blowing the air to the ground near the vehicle. In the other cases the dusty soil was collected and piled near the actual test site, and the air was blown to the pile to generate a dust cloud.

4.1.2 Smoke

Orange smoke was generated with smoke bombs that worked for about one minute. The bomb was held by an assistant, choosing his position so that the wind could carry the smoke cloud towards the space in front of the vehicle. Note that sometimes the direction of the wind varied, forcing the assistant to move to compensate.

4.1.3 Rain in static environment

In the static tests the rain was generated with sprinklers attached to the top of a frame defining the test area (see Fig. 8). This frame covered an area being 9.3 meter long and 4.3 meter wide. The water was stored in a tank equipped with a pump to bring the water to the sprinkler system. This device is visible on the right hand side of the frame and the vehicle.

4.1.4 Rain in dynamic environment

In the dynamic tests the rain was generated with the same tank as in the static tests, but instead of sprinklers, the rain was simulated by spraying water with a hand-held hose pointed at the vehicle's working area.

4.2 Static tests

In the static tests the vehicle was standing still and imaging an area with known features, inside the sprinkler frame used for generating the rain. These objects were generally chosen to be easily detected by the sensors in clear conditions. Most of them are artificial and of simple geometry (e.g. box or pole) and their dimensions are provided: Fig. 7 shows a drawing of this area with locations of the features. However, a branch of tree (attached to a metal bar stuck into the ground) was also set in the test area to have a natural feature. The elements of Fig. 7 are also listed in Table 1 for more details. The positions of these features were chosen so that every sensor (in particular the 2D laser scanners) could see at least some of them and the objects were distributed over the area.

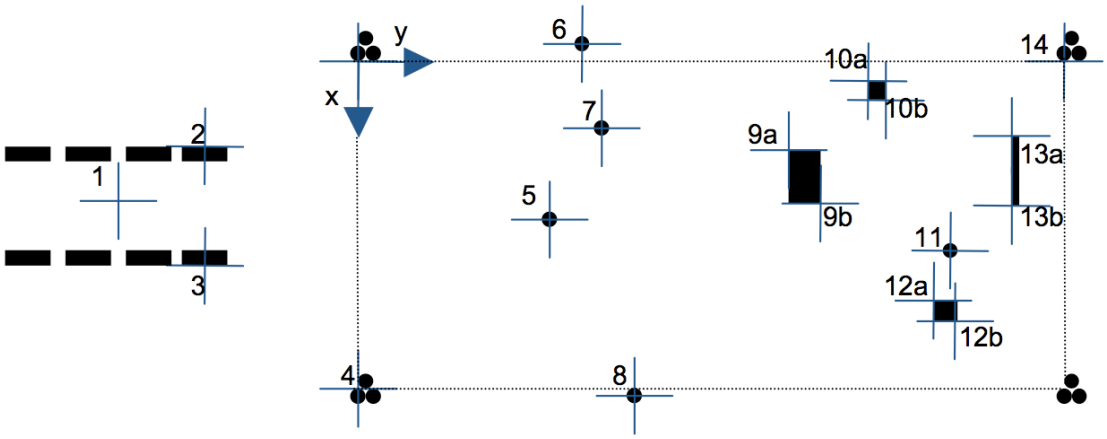

Figure 7: Static trial setup seen from above

The framerate of the visual camera in this series of tests was 15 frames per second, except in the first dataset where the framerate was 10 frames per second.

The vehicle was facing south. Therefore the sun was either behind or on the side of the vehicle (in Australia, where the datasets were collected, the sun shines from the north in the middle of the day). Note that in this section, features mentioned will be located with respect to the vehicle, i.e. *left* will refer to the *Port* side if the Argo, while *right* will refer to its *Starboard* side.

4.2.1 Day 1: Afternoon and evening

The first set of static trials data was acquired on the 15th of October 2008, in the afternoon and in the evening. Most of the datasets were acquired when the sun was above the horizon, except for the last one one (dataset 12), acquired just after sunset. The wind was quite strong, and it affected significantly dust and smoke spreading. It was mainly blowing from the left-hand side of the vehicle.

01-02 - Clear conditions

The first two datasets were acquired in clear conditions, without any artificially created dust, smoke or rain. In dataset 01 the frame rate of the color camera was 10 frames per second, whereas it was 15 frames per second in dataset 02.

Table 1: Elements present in the static trial setup

	Object name	**X (cm)**	**Y (cm)**	**Diam. (cm)**	**Height (cm)**	
origin	Supporting pole of the frame on the left side of Argo	0	0			
1	Centre of Argo sensor frame	190	-293		185	
2	Port front wheel of Argo	112	-202			
3	Starboard front wheel of Argo	269	-202			
4	Supporting pole of the frame on the right side of the Argo	431	0			
5	Tree	108	252	5		(1)
6	Laser pole	-23	295		175	
7	Radar reflector on the top of a pole	88	321		114	(2) **(3)**
8	Laser pole	440	364		175	
9	Two plastic boxes on top of each other: First box	117...187	567...609		33	
	Second plastic box	117...147	578...598		33...67	
10	Brick tower	26...51	672...695		100	
11	Radar reflector on the ground	249	780		29	**(3)**
12	Canister	315...342	758...786		45	
13	Table standing on its side	98...190	861		122	
14	Supporting pole of the frame on the left back side	0	930			

(1) The branch is at the height of 90cm. The foliage of the tree reaches about 120cm to the right.
(2) The radar reflector is hanging so that the top of it is on the top of the supporting pole.
(3) Note that these radar reflectors are present in the test area **only for datasets number 24 to 26**.

Figure 8: Photo of the static trial area (Datasets 01 to 24)

Dataset name: 01-StaticClear-Video10fps

	Unix	UTC	AEDT
Start	1224050945.437	06:09:05.437	15:09:05.437
End	1224051090.447	06:11:30.447	15:11:30.447
Duration	145.010 seconds		

Dataset name: 02-StaticClear-Video15fps

	Unix	UTC	AEDT
Start	1224051487.381	06:18:07.381	15:18:07.381
End	1224051619.116	06:20:19.116	15:20:19.116
Duration	131.735 seconds		

03 - Clear conditions with human

This dataset was acquired in clear conditions, with a human walking (on purpose) through the area (see Fig. 9).

Dataset name: 03-StaticClear-Human

	Unix	UTC	AEDT
Start	1224052418.386	06:33:38.386	17:33:38.386
End	1224052519.662	06:35:20.662	17:35:20.662
Duration	101.276 seconds		

Figure 9: Human walking in the test area during a static test (dataset 03)

04 - Light dust

In this dataset, an assistant blew dust from a pile that was located on the left, out of the test area (Fig. 10). The dust was carried by the wind from left to right. The dust cloud was mainly formed between the sensors and the test area. The dust density was relatively low. The dataset started and ended in clear conditions.

Dataset name: 04-StaticLightDust

	Unix	UTC	AEDT
Start	1224053469.229	06:51:09.229	17:51:09.229
End	1224053602.855	06:53:23.855	17:53:23.855
Duration	133.626 seconds		

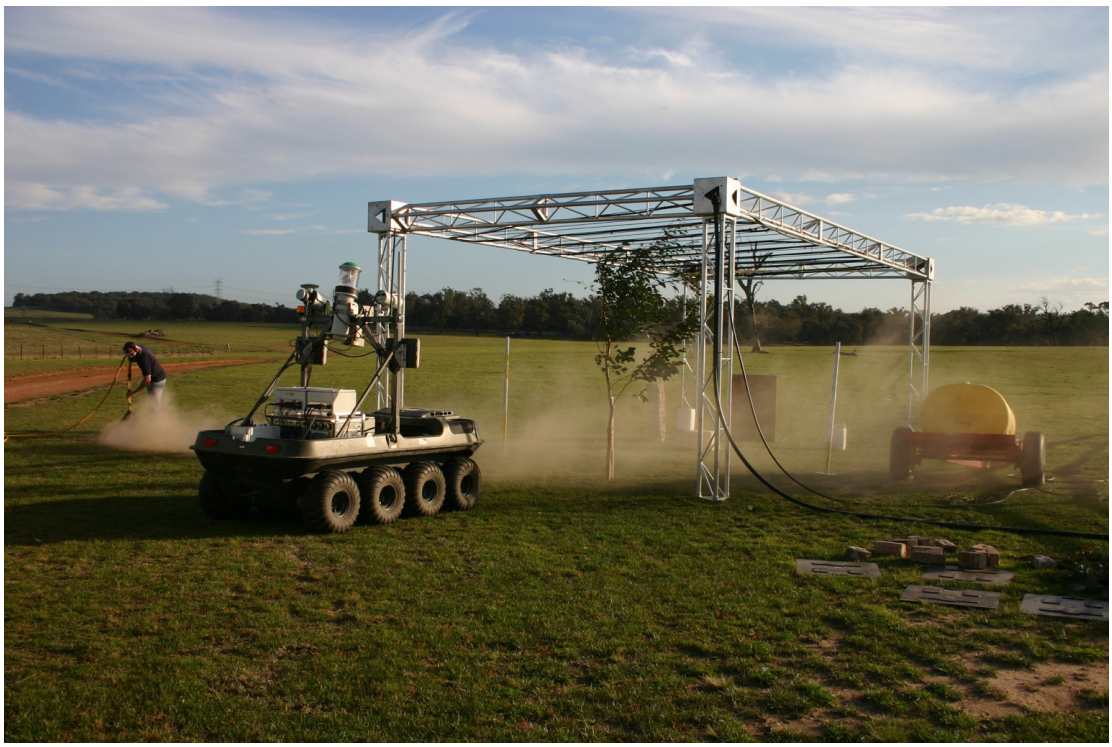

Figure 10: Static test with light dust (dataset 04)

05 - Heavy dust

As previously, in this dataset an assistant blew dust from a pile that was located on the left, out of the test area. The dust was carried by the wind from left to right, and it moved between the sensors and the test area. The dust cloud was denser than in datataset 04. This dataset also started and ended in clear conditions.
Note that the lasers and radar data start 14 to 18 seconds later than the other sensors.

Dataset name: 05-StaticHeavyDust

	Unix	UTC	AEDT
Start	1224054044.006	07:00:44.006	18:00:44.006
End	1224054110.171	07:01:50.171	18:01:50.171
Duration	66.165 seconds		

06 - Light dust with human

As in the two previous cases, an assistant blew dust from a pile that was located on the left of the test area. The dust was carried by wind from left to right. The dust cloud mainly occurred between the sensors and the test area. The dust density was relatively low. A human was walking within the test area. The dataset started and ended in clear conditions.

Dataset name: 06-StaticLightDust-Human

	Unix	UTC	AEDT
Start	1224055857.924	07:30:58.924	18:30:58.924
End	1224055992.320	07:33:12.320	18:33:12.320
Duration	134.396 seconds		

07 - Smoke

An assistant held a smoke bomb at the left of the test area (Fig. 11). The smoke cloud was mostly located between the sensors and the test area. The dataset started and ended in clear conditions.

Dataset name: 07-StaticSmoke

	Unix	UTC	AEDT
Start	1224056457.502	07:40:58.502	18:40:58.502
End	1224056543.290	07:42:23.290	18:42:23.290
Duration	85.788 seconds		

Figure 11: Static test with smoke (dataset 07)

08 - Heavy rain

The sprinklers were used to generate heavy rain. Wind from the left biased the rain towards the right, and therefore the left part of the test area had less rain than the right part. Rain was present during the whole duration of the dataset.

Dataset name: 08-StaticHeavyRain

	Unix	UTC	AEDT
Start	1224056989.625	07:49:50.625	18:49:50.625
End	1224057123.862	07:52:04.862	18:52:04.862
Duration	134.237 seconds		

09 - Heavy rain with human

As before, the sprinklers were used to create heavy rain. A human was walking around the test area. Wind from the left biased the rain towards right again. Rain was present during the whole duration of the dataset.

Dataset name: 09-StaticHeavyRain-Human

	Unix	UTC	AEDT
Start	1224057199.911	07:53:20.911	18:53:20.911
End	1224057280.261	07:54:40.261	18:54:40.261
Duration	80.350 seconds		

10 - Light rain

For this test, water pressure in the sprinklers was reduced to generate lighter rain. As in the previous cases, wind from the left biased the rain towards right with respect to the sensors. The rain was created during the whole duration of the dataset.

Dataset name: 10-StaticLightRain

	Unix	UTC	AEDT
Start	1224057494.661	07:58:15.661	18:58:15.661
End	1224057652.537	08:00:53.537	19:00:53.537
Duration	157.876 seconds		

11 - Clear conditions after rain

In this dataset, the sprinklers were turned off. However, as it was acquired right after the rain datasets, the objects in the test area were still wet, and a few rain drops were still occasionally falling from the top of the frame. The sun was very low but still above the horizon during the acquisition of this dataset.

Dataset name: 11-StaticAfterRainEvening

	Unix	UTC	AEDT
Start	1224057998.295	08:06:38.295	19:06:38.295
End	1224058157.685	08:09:18.685	19:09:18.685
Duration	159.390 seconds		

12 - Clear conditions after rain and sunset

This dataset was acquired just after sunset. There is still reasonable light, but the sun is already below the horizon. This dataset was also acquired shortly after the rain, so all the objects in the test area were still wet, and it is likely that a few drops of water were still falling from the sprinkler system. Note that the lasers data logs stop about 88 seconds before the rest of the data.

Dataset name: 12-StaticClearAfterRainAfterSunset

	Unix	UTC	AEDT
Start	1224058839.207	08:20:39.207	19:20:39.207
End	1224058972.002	08:22:52.002	19:22:52.002
Duration	132.795 seconds		

4.2.2 Day 2: Morning and midday

The second series of static trials was realized on the 16th of October 2008, starting in the morning and lasting until midday. In all of the datasets the sun was high in the sky. There was much less wind than during the first day, but its direction varied.

14 - Clear

This dataset was acquired in clear conditions, without any artificially generated dust, smoke or rain.

Dataset name: 14-StaticMorningClear

	Unix	UTC	AEDT
Start	1224112428.048	23:13:48.048	10:13:48.048
End	1224112600.636	23:16:41.636	10:16:41.636
Duration	172.588 seconds		

15 - Heavy dust

An assistant blew dust from a pile that was located west of the test area. The dust was carried by the wind from left to right. The dust cloud moved slightly to the south-east, therefore the north-eastern corner of the area was not much covered with dust. The dust density was high. The dataset started and ended in clear conditions. Figure 12 shows the dust cloud.

Dataset name: 15-StaticMorningHeavyDust

	Unix	UTC	AEDT
Start	1224113347.161	23:29:07.161	10:29:07.161
End	1224113448.576	23:30:49.576	10:30:49.576
Duration	101.415 seconds		

Figure 12: Static test with heavy dust (dataset 15)

16 - Very light dust

An assistant blew dust from a dusty road west of the test area. Part of the dust was carried by the wind from left to right with. The dust cloud was quite light when reaching the test area. The dataset started and ended in clear conditions.

Dataset name: 16-StaticMorningVeryLightDust

	Unix	UTC	AEDT
Start	1224114064.835	23:41:05.835	10:41:05.835
End	1224114139.801	23:42:20.801	10:42:20.801
Duration	74.966 seconds		

17 - Smoke

An assistant held a smoke bomb that generated smoke in the test area. The wind was weak, but strong enough to carry the smoke cloud towards the test area. The direction of the wind changed during the test. Consequently, the assistant was first standing at the left side of the test area, then he moved to the back and finally to the right side (Fig. 13). However, he was always standing outside of the test area. The dataset started and ended in clear conditions with no smoke.

Dataset name: 17-StaticMorningSmoke

	Unix	UTC	AEDT
Start	1224114471.313	23:47:51.313	10:47:51.313
End	1224114571.005	23:49:31.005	10:49:31.005
Duration	99.692 seconds		

Figure 13: Static test with smoke (dataset 17)

18 - Light rain

The sprinklers were used to generate light rain. The weak wind did not affect much the direction of the rain. Note that the area closer to the sensors did not get as much rain as the area further away. Besides, the rain was not completely uniform in the area, due to a leak in the front.

Dataset name: 18-StaticMorningLightRain

	Unix	UTC	AEDT
Start	1224117868.591	00:44:29.591	11:44:29.591
End	1224117989.562	00:46:30.562	11:46:30.562
Duration	120.971 seconds		

19 - Rain

The sprinklers were used to generate heavier rain. The weak wind did not affect much the direction of the rain.

Dataset name: 19-StaticMorningRain

	Unix	UTC	AEDT
Start	1224120580.504	01:29:41.504	12:29:41.504
End	1224120739.598	01:32:20.598	12:32:20.598
Duration	159.094 seconds		

20 - Smoke

An assistant held a smoke bomb that generated smoke in the test area. In this test the direction of the wind did not change significantly. The assistant was mainly standing at the back-right corner of the test area (Fig. 14). His arm may have entered the test area in the beginning. The dataset started and ended in clear conditions with no smoke. As this dataset was acquired after the rain, all the objects were wet.

Dataset name: 20-StaticMorningSmoke

	Unix	UTC	AEDT
Start	1224120901.096	01:35:01.096	12:35:01.096
End	1224120989.101	01:36:29.101	12:36:29.101
Duration	88.005 seconds		

Figure 14: Static test with smoke (dataset 20)

21 - Clear conditions after rain and smoke

This dataset was acquired after the smoke and rain datasets. Thus, the objects in the test area were still wet, and there might be some residue from the smoke bomb.

Dataset name: 21-StaticMorningClearAfterRainAndSmoke

	Unix	UTC	AEDT
Start	1224121144.696	01:39:05.696	12:39:05.696
End	1224121263.788	01:41:04.788	12:41:04.788
Duration	119.092 seconds		

4.2.3 Day 2: Morning and midday - with added radar reflectors

The second part of the second day's tests was done in the same area, but with two additional features in the area: radar reflectors. Note that their positions are also marked in Fig. 7. Fig. 15 shows the test area with the added radar reflectors.

22 - Clear

The reflectors are in the test area. The dataset was acquired in clear conditions.

Dataset name: 22-StaticMorningClearWithReflectors

	Unix	UTC	AEDT
Start	1224122292.159	01:58:12.159	12:58:12.159
End	1224122430.871	02:00:31.871	13:00:31.871
Duration	138.712 seconds		

23 - Clear, human walking

In this dataset a human was walking in the test area. He did not interact especially with the radar reflectors but walked past them.

Figure 15: Static test area with radar reflectors (Datasets 22 & 23)

Dataset name: 23-StaticMorningClearWithReflectors-Human

	Unix	UTC	AEDT
Start	1224122579.975	02:03:00.975	13:03:00.975
End	1224122682.009	02:04:42.009	13:04:42.009
Duration	102.034 seconds		

24 - Clear, human walking near reflectors

In this dataset the human was also walking in the test area. Unlike for the previous dataset, the walking pattern was meant to be related to the radar reflectors. The human walked near the radar reflectors, first behind the reflector, then between the reflector and the sensors, and finally, on the side of the reflector. This was repeated for both reflectors.

Dataset name: 24-StaticMorningClearWithReflectors-HumanNearReflectors

	Unix	UTC	AEDT
Start	1224122950.838	02:09:11.838	13:09:11.838
End	1224123096.280	02:11:36.280	13:11:36.280
Duration	145.442 seconds		

4.2.4 Summary of *Static* Datasets

The following table summarizes the conditions for each of those datasets gathered with a *static* vehicle.

Dataset	Dust	Smoke	Rain	Human	Comment
01-02					Clear conditions
03				X	
04-05	X				
06	X			X	
07		X			
08			X		
09			X	X	
10			X		
11					Mostly clear (a few rain drops), evening
12					Mostly clear (a few rain drops), after sunset
14					Clear, morning
15-16	X				
17		X			
18-19			X		
20		X			
21					
22					with radar reflectors
23-24				X	with radar reflectors

4.3 Dynamic tests

In the dynamic tests, the vehicle was driving around different areas and acquiring data from the environment. Controlled environmental conditions such as presence of dust, rain and smoke were also generated for some datasets. Unlike for the static datasets, the rain was produced using a mobile equipment.

4.3.1 Open area (*the Triangle*)

The tests in this section were realized in an open area, on mostly flat ground. The soil on the ground was very dusty, which means that rapid movements of the vehicle typically produce dust clouds without any external input. On the northern side of the area is a shed with metal walls. Next to the shed, there is a fence. Another fence is located on the south-western side of the area. Both fences consist of barbed wire and wooden posts. The area is bounded by an unpaved road on the eastern side. Figure 16 is an aerial image of the area. This test area is on the left side of the image. Figure 17 shows a photo of the area.

Figure 16: Aerial image of the *open area* (on the left side of the path) and the *houses area* (on the right side of the path)

29 - Clear conditions during day

This dataset, as all with names between 29 and 32, was acquired during daytime. The vehicle was driving around the area avoiding sharp turns that would have caused much dust.

Figure 17: Photo of the *open area* (Datasets 25 to 32)

Dataset name: 29-DynamicDayTriangleClear

	Unix	UTC	AEDT
Start	1224198733.114	23:12:13.114	10:12:13.114
End	1224199111.326	23:18:31.326	10:18:31.326
Duration	378.212 seconds		

30-31 - Dust during day

These datasets were also acquired during daytime. The vehicle was driving around the area while an assistant was generating the dust. The ground of the area was very dusty, so the large dust clouds could be produced only by pointing a high-pressure blower to the ground (Fig. 18). The assistant needed to walk around the test area. This can be seen in the dataset.

Dataset name: 30-DynamicDayTriangleDust

	Unix	UTC	AEDT
Start	1224199788.106	23:29:48.106	10:29:48.106
End	1224199986.155	23:33:06.155	10:33:06.155
Duration	198.049 seconds		

Dataset name: 31-DynamicDayTriangleMoreDust

	Unix	UTC	AEDT
Start	1224200313.353	23:38:33.353	10:38:33.353
End	1224200500.152	23:41:40.152	10:41:40.152
Duration	186.799 seconds		

32 - Clear conditions after dust on day

This dataset was acquired after the datasets with dust. Thus, the objects in the area are probably more dusty than in the earlier dataset in clear conditions.

Dataset name: 32-DynamicDayTriangleClearAfterDust

	Unix	UTC	AEDT
Start	1224201093.019	23:51:33.019	10:51:33.019
End	1224201271.635	23:54:32.635	10:54:32.635
Duration	178.616 seconds		

Figure 18: Dynamic test in the open area with dust (Datasets 30 & 31)

25-27 - Clear conditions at night with external lights on

These datasets were acquired at nighttime. The sun had set completely, so all the light was artificial. A car was parked in the test area, its headlights were on, pointing towards the area where the Argo vehicle was moving. The UGV's own headlights were also on, illuminating the area in front of it. Note that in dataset 27 the door of the shed was open, with the internal light of the building on. This can be seen in the images of the camera.

Dataset name: 25-DynamicNightClearTriangleWithCarLights

	Unix	UTC	AEDT
Start	1224158167.214	11:56:07.214	22:56:07.214
End	1224158524.566	12:02:05.566	23:02:05.566
Duration	357.352 seconds		

Dataset name: 27-DynamicNightClearTriangleWithCarLights2

	Unix	UTC	AEDT
Start	1224159874.355	12:24:34.355	23:24:34.355
End	1224160153.568	12:29:14.568	23:29:14.568
Duration	279.213 seconds		

26-28 - Clear conditions at night without external lights

These datasets were acquired at nighttime, the only artificial light coming from the UGV's own headlights (i.e. in particular, the car's lights were turned off this time).

Dataset name: 26-DynamicNightClearTriangleNoCarLights

	Unix	UTC	AEDT
Start	1224158859.005	12:07:39.005	23:07:39.005
End	1224159161.470	12:12:41.470	23:12:41.470
Duration	302.465 seconds		

Dataset name: 28-DynamicNightClearTriangleNoCarLights2

	Unix	UTC	AEDT
Start	1224160333.789	12:32:14.789	23:32:14.789
End	1224160606.918	12:36:47.918	23:36:47.918
Duration	273.129 seconds		

Summary

The following table summarizes the conditions for each of these datasets gathered in the *open area* (also called the *Triangle*).

Dataset	Dust	Daytime	Night w. Ext. Light	Night no Ext. Light	Comment
29		X			Clear
30-31	X	X			
32		X			After dust
25 & 27			X		with car lights
26 & 28				X	

4.3.2 Houses area

This is an area with three wooden buildings. A long building is standing in the southern side of the area. Two smaller ones are on the northern side. The whole area is bounded by a fence. This houses area can be seen on the right side of the aerial image in Fig. 16.

33 - Clear conditions without humans

This dataset was acquired at daytime. The vehicle was driving around the area with houses (see Fig. 19).

Dataset name: 33-DynamicDayHousesClear

	Unix	UTC	AEDT
Start	1224201950.093	00:05:50.093	11:05:50.093
End	1224202213.225	00:10:13.225	11:10:13.225
Duration	263.132 seconds		

Figure 19: Dynamic test around the houses (Datasets 33 & 34)

34 - Clear conditions, human walking around

This dataset was also acquired at daytime. The vehicle was driving around the same area as before and in similar conditions. However, in addition to the previous dataset, a human was walking around during the test.

Dataset name: 34-DynamicDayHouses-Human

	Unix	UTC	AEDT
Start	1224202880.040	00:21:20.040	11:21:20.040
End	1224203087.626	00:24:48.626	11:24:48.626
Duration	207.586 seconds		

4.3.3 Area with trees and water (*dam area*)

This is an area next to a lake. On the southern side of the area stands a small eucalyptus forest. A photo of the area is shown in Fig. 20. For convenience, this area will be called the *Dam area*.

Figure 20: Photo of the *dam area* (Datasets 35 to 40)

35 - Clear conditions

This dataset, as all between 35 and 40, was acquired at daytime. The vehicle was driving around the dam area.

Dataset name: 35-DynamicDayDamClear

	Unix	UTC	AEDT
Start	1224216067.282	04:01:07.282	15:01:07.282
End	1224216412.990	04:06:53.990	15:06:53.990
Duration	345.708 seconds		

36-37 - Dust

In this test, an assistant was generating dust by pointing the blower to the ground. It was not as dusty as in the open area, therefore the dust cloud was lighter in this area. The assistant had to slightly change positions occasionally in order to have the dust cloud most of the time in front of the vehicle. Figure 21 shows a photo of the actual situation.

Dataset name: 36-DynamicDayDamDust

	Unix	UTC	AEDT
Start	1224216779.827	04:13:00.827	15:13:00.827
End	1224216962.271	04:16:02.271	15:16:02.271
Duration	182.444 seconds		

Dataset name: 37-DynamicDayDamDust2

	Unix	UTC	AEDT
Start	1224217352.224	04:22:32.224	15:22:32.224
End	1224217563.883	04:26:04.883	15:26:04.883
Duration	211.659 seconds		

Figure 21: Dynamic test in the dam area with dust (Datasets 36 to 37)

38 - Smoke

An assistant held a smoke bomb, trying to stay in a position where the smoke went towards the vehicle, which involved changing position. Fig. 22 shows a photo of the situation. The photo was taken by the assistant holding the smoke bomb.

Dataset name: 38-DynamicDayDamSmoke

	Unix	UTC	AEDT
Start	1224217939.781	04:32:20.781	15:32:20.781
End	1224218021.286	04:33:41.286	15:33:41.286
Duration	81.505 seconds		

39 - Rain

This dataset was acquired at daytime. An assistant created a “water curtain” in front of the vehicle with a hose spraying water. Once again, the assistant had to move to keep the water in front of the vehicle. Fig. 23 shows a photo of the situation.

Figure 22: Dynamic test in the dam area with smoke (Dataset 38)

Dataset name: 39-DynamicDayDamRain

	Unix	UTC	AEDT
Start	1224229665.084	07:47:45.084	18:47:45.084
End	1224229783.877	07:49:44.877	18:49:44.877
Duration	118.793 seconds		

40 - Clear, sun low in the sky

This dataset was acquired in the evening, just before the sunset. No artificial adverse environmental condition was generated in this test and nobody was moving around.

Dataset name: 40-DynamicDayDamClearSunLow

	Unix	UTC	AEDT
Start	1224230071.163	07:54:31.163	18:54:31.163
End	1224230243.984	07:57:24.984	18:57:24.984
Duration	172.821 seconds		

Summary

The following table summarizes the environmental conditions for each of those datasets gathered in the *dam area*.

Dataset	Dust	Smoke	Rain	Comment
35				Clear
36-37	X			
38		X		
39			X	
40				Clear, sun low

4.3.4 Summary of *Dynamic* Datasets

The following table shows a summary of all conditions covered in all *dynamic* datasets. It does not precise the area in which the dataset was acquired though, this precision can be found directly in the ap-

Figure 23: Dynamic test in the dam area with simulated rain (Dataset 39)

propriate section. The default configuration is at daytime (i.e. **Night** is only precised where appropriate).

Dataset	Dust	Smoke	Rain	Human	Night	Area	Comment
25 to 28					X	Open area	Clear, at night
29 & 32						Idem	Clear
30 & 31	X					Id.	
33						Houses area	Clear
34				X		Id.	
35						Dam area	Clear
36 & 37	X					Id.	
38		X				Id.	
39			X			Id.	
40						Id.	Clear

4.4 Calibration Datasets

4.4.1 Cameras

The data used to realize the calibrations concerning the Visual camera and the IR camera can be found respectively in the directories `VisualCameraCalibration` and `IRcameraCalibration`, which are both organised as follow. They contain the following directories:

- `LaserHorizontal`
- `LaserPort`
- `LaserStarboard`
- `LaserVertical`
- `VideoVisual` or `VideoIR` as appropriate

which content is as described for the other datasets (see section 3.2).

In an additional directory, named `Calibration`, the following files and directories can be found:

- `Calib_Results.m` and `Calib_Results.mat` are the files exported by the Matlab Calibration Toolbox, containing all the estimated calibration parameters.

- `Images` is a directory containing the images that were used for the camera calibration process, named with successive numbers starting by 1, for convenience when loading them into Matlab.
- `matlabAsciiLaserData` is a directory containing the ascii descriptions of all laser data in files formatted to be suitable for Matlab, for convenience.
- `VideoLogAsciiCalibration.txt` is a text file figuring the timestamps for all images in `Images`. The line number in this file corresponds to image number as it is named in `Images` (e.g. the timestamp corresponding to the image named `image002.bmp` can be found at line number 2 of `VideoLogAsciiCalibration.txt`).

The images in these datasets show a chess board exposed with various orientations in space, and at various distances. Note that these chess boards *are different for the Visual camera and the IR camera*. The size of the Black and White squares of these chess board are the following:

- for the IR camera: $114.8mm$ on both sides.
- for the Visual camera: $74.9mm$ on the axis *left-right* as it can be seen in the images and $74.7mm$ on the axis corresponding to the direction *up-down*.

4.4.2 Range Sensors (Lasers and Radar)

The data used for the range sensors calibration can be found in the directory named:

`RangeSensorsCalibration`

It is organized exactly as the regular datasets that were presented before, except that it does not contain the directories `RadarSpectrum` and `Payload`. For this dataset, data from all sensors were collected in the *open area*, with four vertical poles standing on a flat ground. These special features of known geometry as well as the vertical wall of the shed and the flat part of the ground were used to extract relevant data for the calibration process [1, 9].

4.5 List of all Datasets

The following list shows the names of all datasets mentioned in this report, i.e. the names of all directories containing sensor data:

- `01-StaticClear-Video10fps`
- `02-StaticClear-Video15fps`
- `03-StaticClear-Human`
- `04-StaticLightDust`
- `05-StaticHeavyDust`
- `06-StaticLightDust-Human`
- `07-StaticSmoke`
- `08-StaticHeavyRain`
- `09-StaticHeavyRain-Human`
- `10-StaticLightRain`
- `11-StaticAfterRainEvening`
- `12-StaticClearAfterRainAfterSunset`
- `14-StaticMorningClear`
- `15-StaticMorningHeavyDust`
- `16-StaticMorningVeryLightDust`
- `17-StaticMorningSmoke`

- 18-StaticMorningLightRain
- 19-StaticMorningRain
- 20-StaticMorningSmoke
- 21-StaticMorningClearAfterRainAndSmoke
- 22-StaticMorningClearWithReflectors
- 23-StaticMorningClearWithReflectors-Human
- 24-StaticMorningClearWithReflectors-HumanNearReflectors
- 25-DynamicNightClearTriangleWithCarLights
- 26-DynamicNightClearTriangleNoCarLights
- 27-DynamicNightClearTriangleWithCarLights2
- 28-DynamicNightClearTriangleNoCarLights2
- 29-DynamicDayTriangleClear
- 30-DynamicDayTriangleDust
- 31-DynamicDayTriangleMoreDust
- 32-DynamicDayTriangleClearAfterDust
- 33-DynamicDayHousesClear
- 34-DynamicDayHouses-Human
- 35-DynamicDayDamClear
- 36-DynamicDayDamDust
- 37-DynamicDayDamDust2
- 38-DynamicDayDamSmoke
- 39-DynamicDayDamRain
- 40-DynamicDayDamClearSunLow
- VisualCameraCalibration
- IRcameraCalibration
- RangeSensorsCalibration

5 Preliminary Analysis

This chapter proposes illustrations of the performance of the sensors considered in this work, in the presence of challenging conditions. It is based on the *static* datasets, to allow direct comparisons between sensors and variable conditions.

Figures with legend have been prepared to ease the interpretation of laser scans that will be shown in this document. Fig. 24 presents the correspondances between objects in the scene as perceived by the on-board colour camera and a single laser scan (displayed as range function of angle), in *clear* conditions (dataset 02). Note that for convenience, all laser and radar scans displayed in this chapter will show only the range of angles corresponding to the perception of the test area. Similarly, the correspondances in the LaserPort and LaserStarboard scans are visible in Fig. 25.

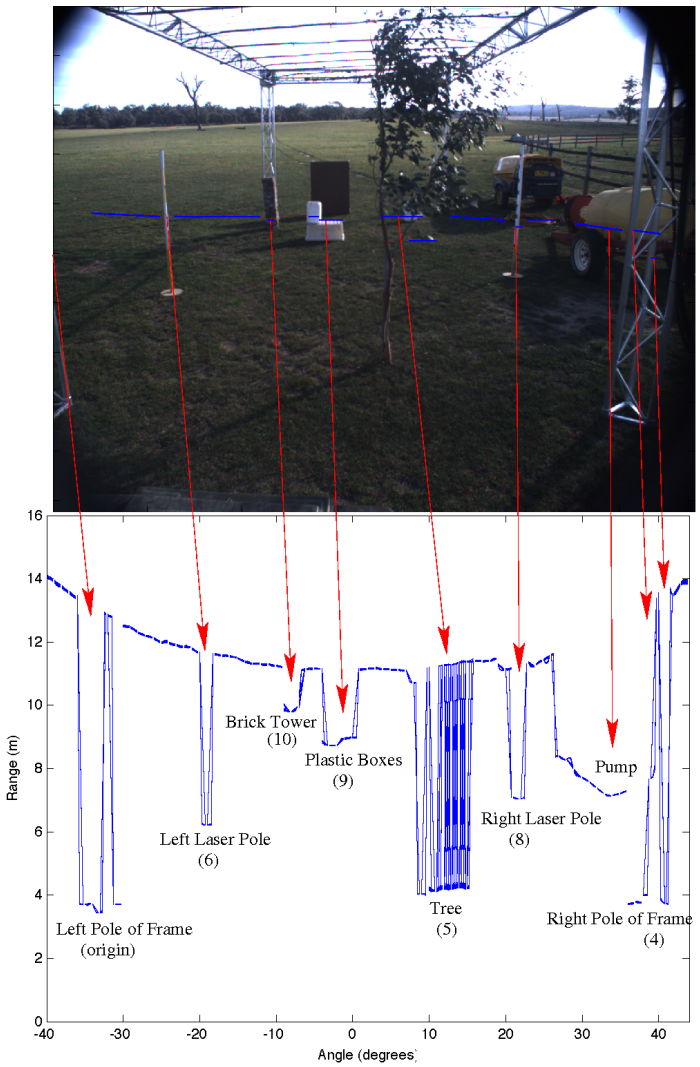

Figure 24: Colour image of the static scene (above) from the Visual Camera and the corresponding *LaserHorizontal* scan display (below), in *clear* conditions, over the 2 minute complete dataset 02 (displayed with solid lines).

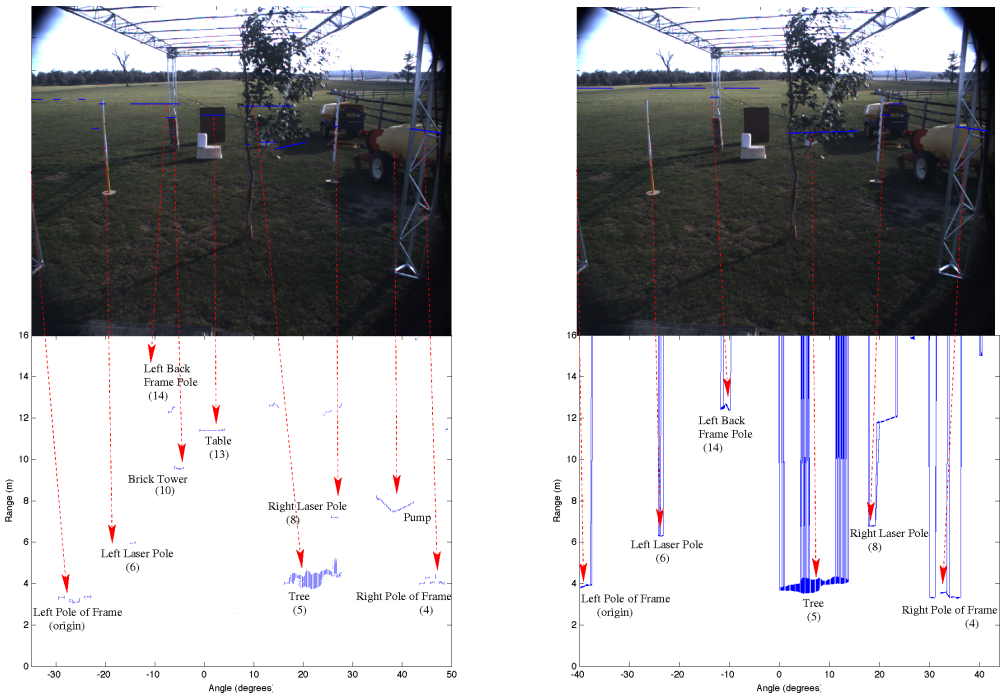

(a) *LaserPort* (b) *LaserStarboard*

Figure 25: Colour image of the static scene (above) from the Visual Camera and the corresponding *LaserPort* (a) and *LaserStarboard* (b) scan displays (below), in *clear* conditions, over the 2 minute complete dataset 02.

5.1 Effect of Dust/Smoke on Range Sensors (Lasers and Radar)

Lasers are extremely affected by dust and smoke. More precisely, a cloud of dust or smoke is almost seen as an actual obstacle. Thus, a basic interpretation of the data provided by them might lead to *false detection* of large obstacles. This is all the more true as the SICK lasers only provide the information concerning the *first* return [12].

The radar operates at *mm* wavelengths, which makes the size of dust and smoke particles relatively much smaller, giving radar waves more penetration. Consequently, it is much less affected by dust or smoke, except for a slight increase of the level of noise in the data, and lower reflectivities for the returns. The following figures illustrate those statements.

Fig. 26 and 27 show all the range values returned by the *LaserHorizontal* and the radar respectively, for a static test in clear conditions (dataset 02). All scans made during the complete duration of the dataset collection are drawn in these figures. The angle range corresponds to what is perceived in the test area: the first and last notable feature on the left and right of the graph are respectively the left and right poles of the trial frame (objects labelled *origin* and (4) in table 1 and Fig. 7). Note that the laser, providing much more precise (raw) range measurements than the radar, detects all the objects that are located in its field of view, while the radar detects only the main ones and provides noiser data.

Fig. 28 shows the same measurements from the *LaserHorizontal* and radar in the presence of dust (dataset 05). We can see that dust generates random points in the laser scans, located between the vehicle and the actual position of the obstacle, whereas the range measurements from the radar are not visibly affected. A similar observation can be made on the other lasers scans, such as *LaserPort* and *LaserStarboard* (see Fig. 29).

Fig. 30 shows that the results are similar in the presence of smoke: the laser detects it as it would detect an actual obstacle whereas the radar data are not significantly affected.

5.2 Effect of Rain on Range Sensors (Lasers and Radar)

On Fig. 31 and 32 we can have a preliminary view of the effect of rain on the range measurements from lasers and radar scans. Note that laser scans displayed in this section are all from the *LaserHorizontal*.

[12] some other laser scanners also provide information about possible additional returns. This might at least lead to some suspicion on the features perceived with a significant difference between these returns.

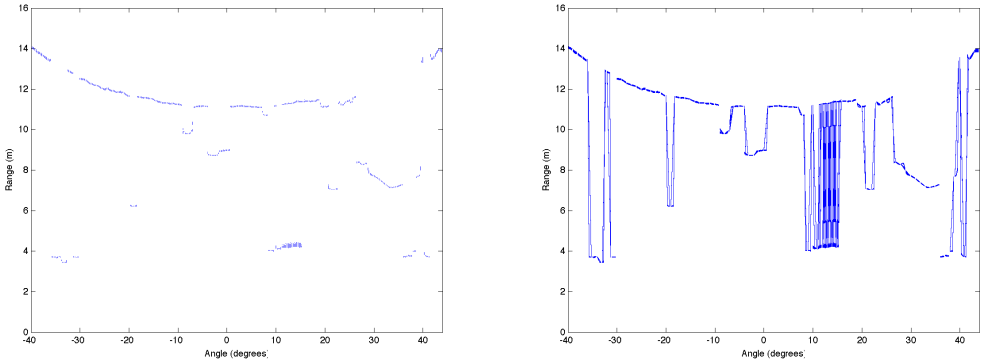

(a) Dots display (b) Lines display

Figure 26: Range returned by *LaserHorizontal* over angle, for static test in clear conditions (dataset 02); displayed in dots in (a) and lines in (b)

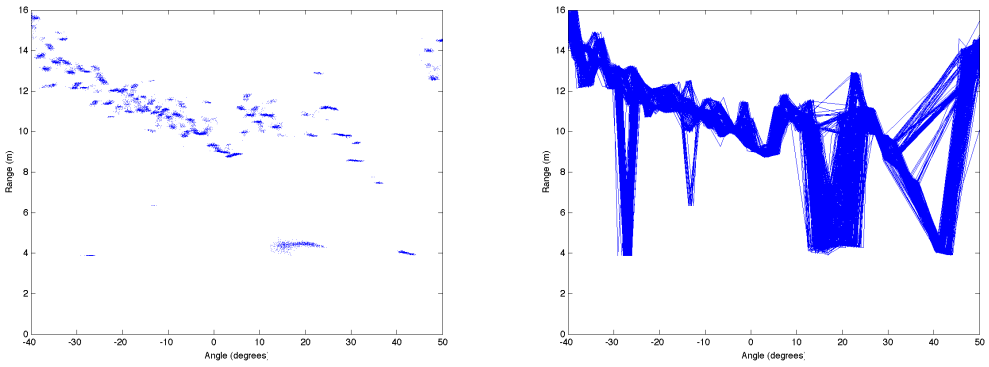

(a) Dots display (b) Lines display

Figure 27: Range returned by the radar (`RadarRangeBearing`) over angle, for static test in clear conditions (dataset 02); displayed in dots in (a) and lines in (b)

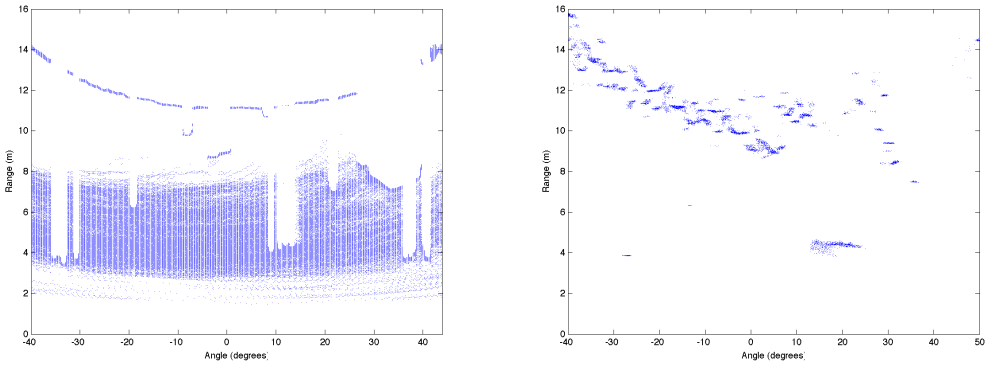

(a) *LaserHorizontal* (b) Radar

Figure 28: Range returned by *LaserHorizontal* and the radar (`RadarRangeBearing`) over angle, for static test with *heavy dust* (dataset 05).

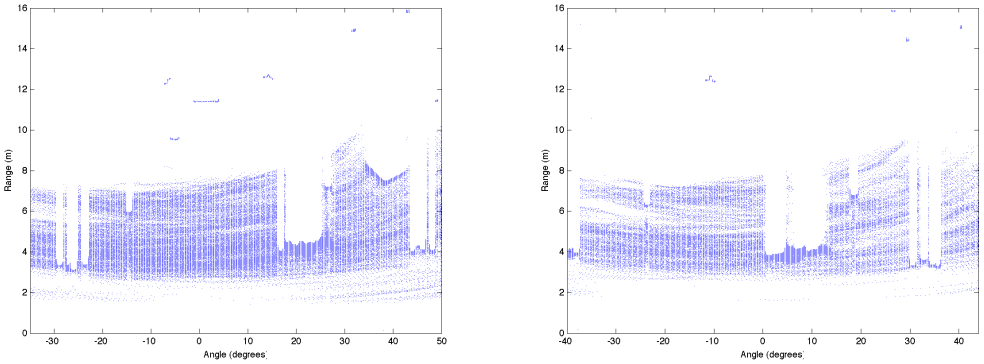

(a) LaserPort (b) LaserStarboard

Figure 29: Range returned by *LaserPort* and *LaserStarboard* over angle, for static test with *heavy dust* (dataset 05).

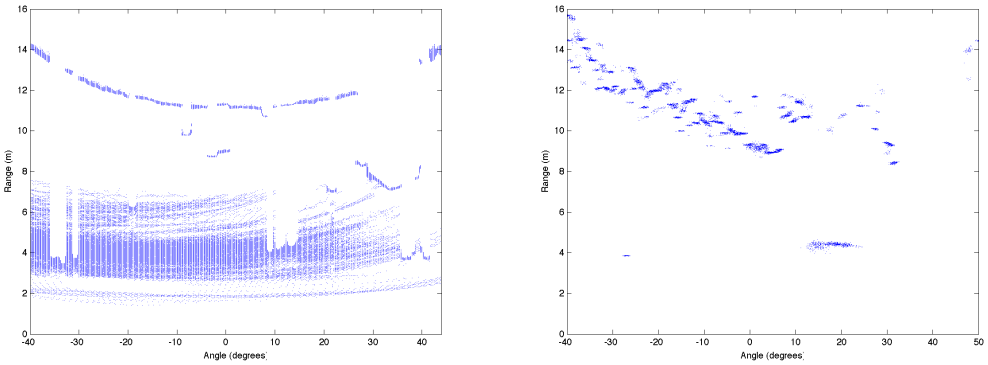

(a) *LaserHorizontal* (b) Radar

Figure 30: Range returned by the *laserHorizontal* and the radar over angle, for static test with *smoke* (dataset 07).

However, similar effects are observed on the other laser scans.

The laser data appear not to be significantly affected by rain, except for a small number of isolated returns from otherwise empty space. These are thought to be laser returns from specific rain drops. Note that these points are isolated, spatially and temporally. Fig. 33 shows another illustration of this phenomenon, using dataset 11. Although this dataset was labelled as *clear conditions*, since the rain test was realized just a few minutes before, there were still some rain drops falling from the sprinklers, some being probably of larger volume than in the rain-labelled tests.

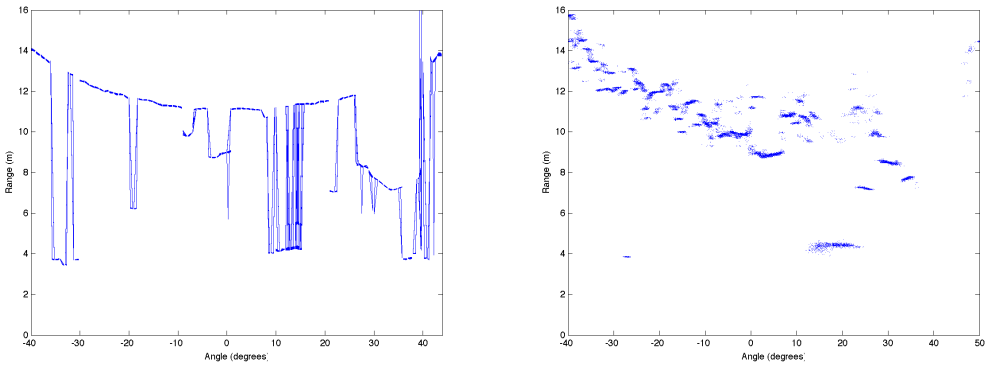

(a) *LaserHorizontal* (b) Radar

Figure 31: Range returned by the *laserHorizontal* and the radar over angle, for static test with *heavy rain* (dataset 08). The laser scan is drawn with lines for an easier identification of outliers, which are isolated returns from otherwise empty space, probably due to specific rain drops (compare with Fig. 26 (b)).

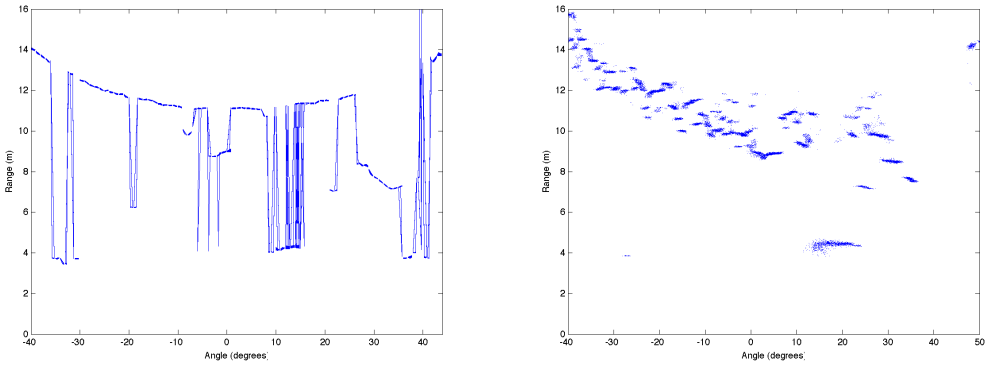

(a) *LaserHorizontal* (b) Radar

Figure 32: Range returned by the *laserHorizontal* and the radar over angle, for static test with *light rain* (dataset 10). The Laser data is here drawn with lines for an easier identification of outliers, which are isolated returns from otherwise empty space, probably due to specific rain drops (compare with Fig. 26 (b)).

5.3 Effect of Dust/Smoke on Camera Images

Both visual and IR camera images are affected by dust (and smoke), but the effect is lower on the infra-red data, as infra-red waves have a higher penetration power. Fig. 34(a) shows the evolution in time of the R,G,B information of one specific line of the images captured by the colour camera (shown in black in Fig. 34(b)), over a complete dataset 07, in the presence of smoke.

To further illustrate the effect of dust on visual information, the R,G,B signals over a specific line (corresponding roughly to the intersection of the *LaserHorizontal* scan plane with the visual image) have been displayed for a single image in Fig. 35 and then over all the images of some chosen datasets. Fig. 36 shows the signals in clear conditions: the level of noise over time in each of the three signals cannot be

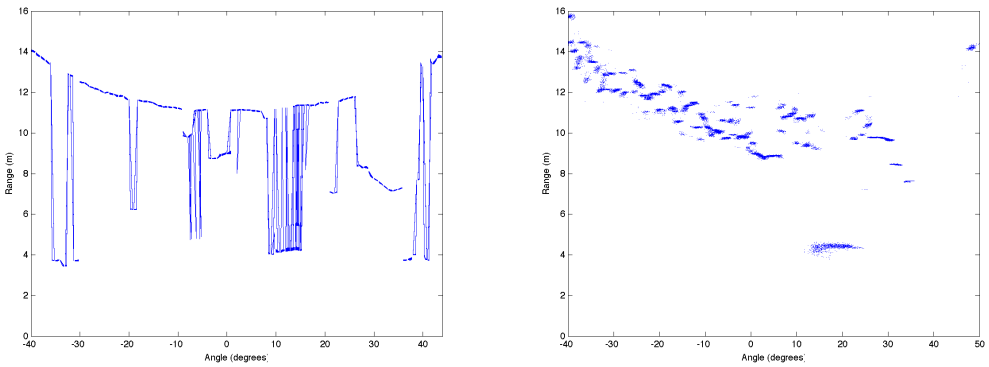

(a) *LaserHorizontal* (b) Radar

Figure 33: Range returned by the laserHorizontal and the radar over angle, for static test with *clear conditions after rain* (dataset 11). The Laser data is here drawn with lines for an easier identification of outliers, due to specific rain drops (compare with Fig. 26 (b)). Note that if the "rain generator" sprinklers were turned off for this dataset, as the data were gathered only a few minutes after dataset 10, some rain drops still remained.

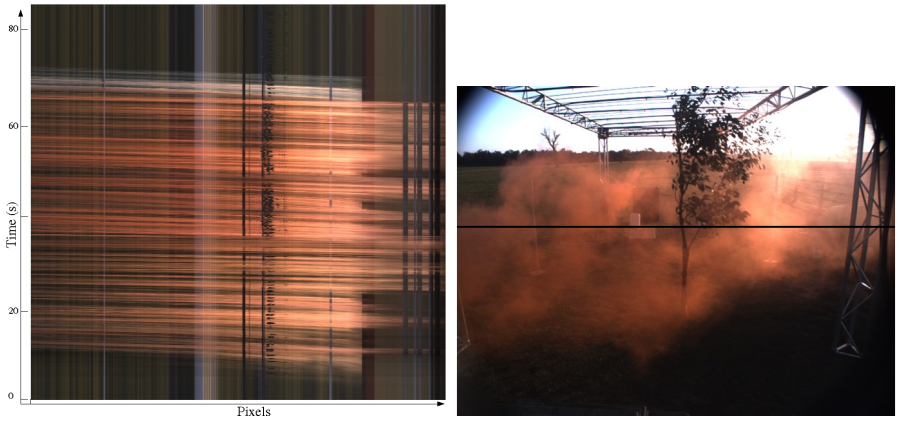

(a) Line over time (b) Colour image at $(t = 39.5s)$

Figure 34: Evolution of one RGB line of the colour images (in black in (b)) over time, in the presence of smoke (dataset 07).

neglected, but it is still a relatively simple task to identify features in the environment. Fig. 37 and Fig. 38 show how much these signals are affected by dust and smoke, respectively. In these conditions, especially in the presence of smoke, it seems practically almost impossible to identify the features in the environment that are behind the dust/smoke cloud.

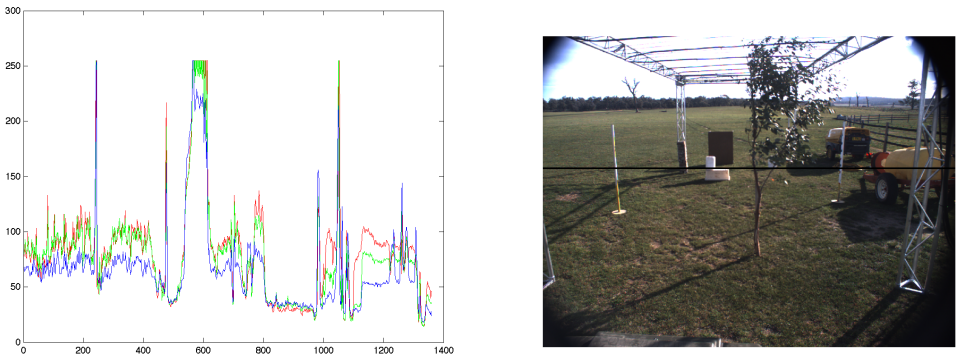

(a) R,G,B signals over the line (b) The original image (line in black)

Figure 35: The R,G,B values (a) over the line indicated in black in the original image (b)

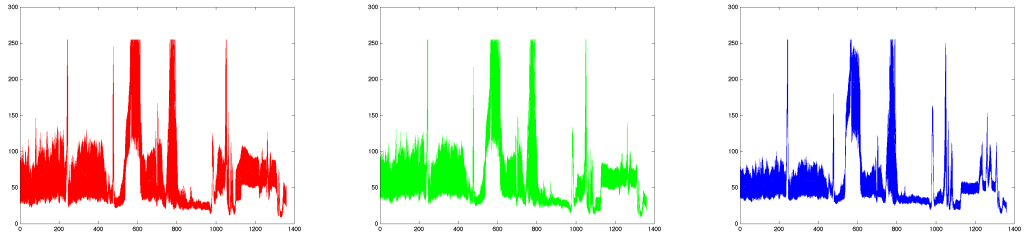

(a) R (b) G (c) B

Figure 36: The R,G,B values for the line indicated in Fig. 35, over the complete (2 minute long) dataset 02, in clear conditions.

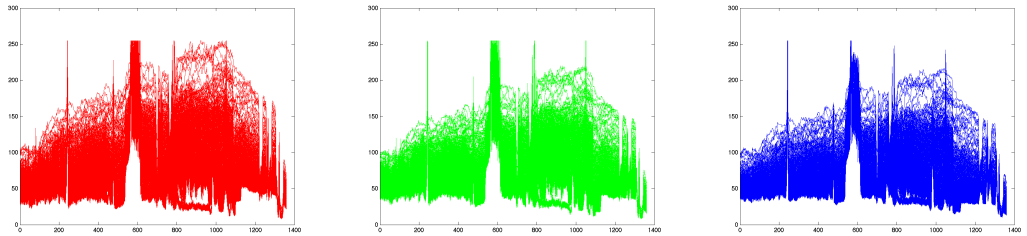

(a) R (b) G (c) B

Figure 37: The R,G,B values for the line indicated in Fig. 35, over the complete (1 minute long) dataset 05, in the presence of dust.

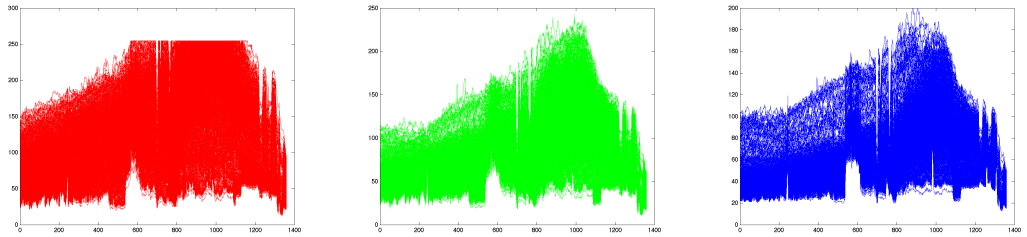

(a) R (b) G (c) B

Figure 38: The R,G,B values for the line indicated in Fig. 35, over the complete (85s long) dataset 07, in the presence of smoke.

References

[1] A. Alempijevic, S.R. Kodagoda, J.P. Underwood, S. Kumar, and G. Dissanayake. Mutual information based sensor registration and calibration. In *Procedings of the 2006 IEEE/RSJ Int. Conf. on Intelligent Robots and Systems*, 2006.

[2] Jean-Yves Bouguet. *Camera Calibration Toolbox for Matlab*. http://www.vision.caltech.edu/bouguetj/calib_doc/.

[3] Ross Hennessy. A generic architecture for scanning range sensors. Master's thesis, The University of Sydney, 2005.

[4] Andrea Monteriu, Prateek Asthan, Kimon Valavanis, and Sauro Longhi. Model-based sensor fault detection and isolation system for unmanned ground vehicles: Experimental validation (part ii). In *2007 IEEE International Conference on Robotics and Automation*, 2007.

[5] Andrea Monteriu, Prateek Asthan, Kimon Valavanis, and Sauro Longhi. Model-based sensor fault detection and isolation system for unmanned ground vehicles: Theoretical aspects (part i). In *2007 IEEE International Conference on Robotics and Automation*, 2007.

[6] T. Peynot and S. Lacroix. Selection and monitoring of navigation modes for an autonomous rover. In *10th International Symposium on Experimental Robotics 2006 (ISER '06)*, 2006.

[7] Robert Pless and Qilong Zhang. Extrinsic calibration of a camera and laser range finder. Technical report, Washington University in St. Louis, 2003.

[8] Prosilica. *GigE Vision Cameras for Machine Vision*. http://www.prosilica.com/support/gige/ge_controls.html, 2006-2008.

[9] James Underwood, Andrew Hill, and Steven Scheding. Calibration of range sensor pose on mobile platforms. In *Procedings of the 2007 IEEE/RSJ Int. Conf. on Intelligent Robots and Systems*, 2007.